

Dual Fluorescent Photochromic Colorants Bearing Pyrano[3,2-*c*]chromen-5-one MoietyChao-Chen Lin,[†] Cheng-Chih Hsieh,[†] Ya-Chien Yu,[†] Chin-Hung Lai,[†] Chin-Neng Huang,[‡] Pei-Yu Kuo,[‡] Chi-Hui Lin,[‡] Ding-Yah Yang,^{*,‡} and Pi-Tai Chou^{*,†}*Department of Chemistry, National Taiwan University, 106 Taipei, Taiwan, and Department of Chemistry, Tunghai University, 407 Taichung, Taiwan**Received: April 30, 2009; Revised Manuscript Received: July 7, 2009*

In this study, the photochromic processes of 8-*N,N*-dimethylamino-2,2-dimethyl-2*H*-pyrano[3,2-*c*]chromen-5-one (**1**) and its derivatives (**2**, **3**) are investigated with steady-state, temperature-dependent and time-resolved absorption and emission spectroscopy. The differences among compounds **1**–**3** lie in their various substituents anchored at the pyran moiety that is subject to the photoinduced ring-opening reaction. Compounds **1** and **2** exhibit salient photochromism with a very unique phenomenon, in which fluorescence is observed in **1** for both the ring-closed form (**1-CF**, $\lambda_{\max} \approx 445$ nm) and the ring-open form (**1-OF**, $\lambda_{\max} \approx 650$ nm in CH₂Cl₂). The yields of forward and reverse photochromism processes were determined to be 0.40 and 1.0% for **1**. Along with fluorescence quantum yields of 9.5×10^{-2} and 5.8×10^{-3} for **1-CF** and **1-OF**, respectively, **1** enables fluorescence detection while it exhibits photochromism in both directions, that is, a photoinduced on/off fluorescence switch. An increase in on/off ratiometric fluorescence between **1-OF** and **1-CF** can reach a factor of 4.0 upon excitation at the absorption isosbestic point. The activation energies for the ground-state **OF**_{trans} → **CF** thermal bleaching processes were determined to be 58.2 and 54.8 kJ/mol, with frequency factors of 1.7×10^5 and 3.6×10^5 s⁻¹ for **1** and **2**, respectively. Conversely, bromo-substituted **3** did not undergo photochromic reaction, as evidenced by the lack of changes in the absorption spectrum after a prolonged (2 h) 354 nm (0.2 W/cm²) photolysis, manifesting the fact that other relaxation processes, such as enhanced intersystem crossing, may govern the deactivation of **3** (**3-CF**) upon excitation.

1. Introduction

Organic photochromic compounds, which are converted from colorless to colored forms upon UV irradiation, have long attracted attention because of their potential applications in optical switching and optical storage.¹ Among them, spiropyrans and naphthopyrans (or chromenes) are widely investigated.^{2–7} UV light of suitable energy facilitates the cleavage of the C–O bond on the pyran moiety, leading to ring-opening. Absorption spectrum of the ring-open form (OF) generally extends to the visible region because the conjugation is elongated relative to the ring-closed form (CF).⁸ The OF product undergoes thermal bleaching and transforms back to CF when placed in the dark. Whereas modifications of existing photochromes to achieve superior photochromic properties are still of current interest, developing new classes of organic photochromic dyes is also important, aiming at gaining insight into the fundamental mechanism and prospective practical applications. Bearing this in mind, we have recently designed a new photochromic colorant that possesses oxazabicyclic moiety, for which the novel ring-opening reaction paved another avenue for the development of photochromic dyes.⁹

We also realized that emission, having zero background in theory, should be much more sensitive than absorption changes. However, photochromism commonly occurs through a nonadiabatic process, that is, crossing to a ground-state potential energy surface (PES) after excitation relaxation. Consequently, the associated fluorescence is rarely observed regarding pho-

tochromic colorants,^{10,11} until very recently, an elegant case of dual fluorescence photochromes was reported on the basis of diarylethene moieties,¹² among which the most strongly fluorescent compound in the series exhibited quantum yields of 0.114 and 0.009 for each isomer.

To continue our efforts on fundamental and applications of photochromism, in our subsequent study, a new class of organic photochromic compounds bearing a coumarin chromophore as the potential fluorescent unit was strategically designed.⁹ Unfortunately, despite the anchored coumarin moiety, similar to most photochromic colorants, these compounds were essentially nonluminescent because of negligible contribution of the coumarin moiety to either HOMO or LUMO in the lowest-lying transition.⁹ For further advancement, our effort then focused on utilization of other fluorescence-based coumarin analogues. Strategically, the second generation has been designed such that the photochromic site is directly attached to the coumarin chromophore.¹³ Herein, we report the comprehensive investigation of the photochromic colorant 8-*N,N*-dimethylamino-2,2-dimethyl-2*H*-pyrano[3,2-*c*]chromen-5-one¹³ (compound **1**; **1-CF** and **1-OF** denote the closed and open forms, respectively; see Scheme 1) and its analogous derivatives **2** and **3** (Scheme 1). In particular, **1** (or **2**) exhibits salient photochromism with a very unique phenomenon in which fluorescence is observed for both **1-CF** and **1-OF** forms. Detailed results and discussion of thermodynamics as well as reaction kinetics are described in the following sections.

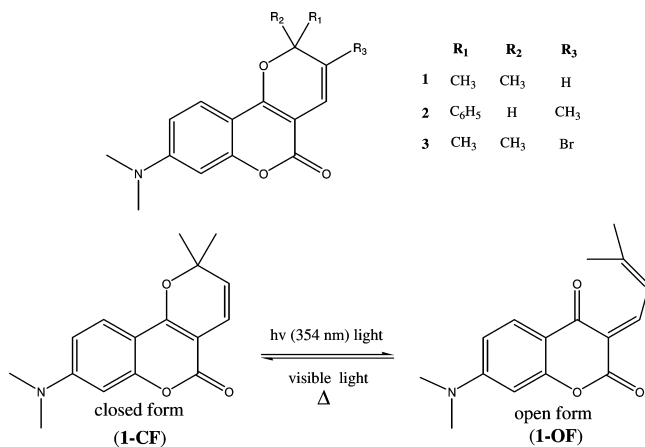
2. Experimental Section

2.1. Synthesis of 1-CF and its Derivatives. Synthesis of **1-CF** and **2-OF** was conducted according to the procedures reported previously.¹³ Briefly, 3-methyl-2-butenal or (*E*)-2-

* Corresponding authors. E-mail: chop@ntu.edu.tw (P.-T.C.); yang@thu.edu.tw (Y.Y.).

[†] National Taiwan University.

[‡] Tunghai University.

SCHEME 1: Structures of Compounds 1–3 and the Photochromism Reaction Illustrated by Compound 1

methyl-3-phenylacrylaldehyde along with a catalytic amount of ethylenediammonium diacetate were added to a solution of 7-*N,N*-dimethylamino-4-hydroxycoumarin in the mixture of CH₂Cl₂ and CH₃OH. After the mixture was stirred at room temperature for 3 h, water was added, and the product was extracted twice with CH₂Cl₂. The combined organic extracts were dried over MgSO₄, filtered, and concentrated. The resulting crude product was then purified by column chromatography. As for **3-CF**, FeBr₃ and bromine were added to a solution of **1-CF** in CH₂Cl₂. After the mixture was stirred at room temperature for 4 h, water was added to quench the reaction, and the product was extracted and purified using the same procedures as those of **1-CF**. The solvents were of reagent grade (Aldrich) and dried prior to use.

2.2. Measurements. Steady-state absorption and emission spectra were recorded by a Hitachi (U-3310) spectrophotometer and an Edinburgh (FS920) fluorimeter, respectively. The various solvents were of spectragrade quality (Merck) and were used right after being received. Coumarin 480 ($\lambda_{em} = 471$ nm, Exciton) in ethanol and DCM (4-(dicyanomethylene)-2-methyl-6-(*p*-dimethylaminostyryl)-4*H*-pyran, $\lambda_{em} = 615$ nm, Exciton) in methanol, with Φ of 0.95 and 0.43, served as the reference for measuring emission quantum yields.^{14a,b} Emission quantum yields were calculated using

$$QY_s = QY_r \frac{I_s A_r n_s^2}{I_r A_s n_r^2} \quad (1)$$

by comparing the integrated areas (I , where the subscripts s and r denote sample and reference respectively) under the fluorescence curves with similar absorbance (A) at the same excitation wavelength and were corrected for the refractive indices (n) of the solvents used.^{14c}

A variable temperature unit (Specac, P/N 21525) was used to carry out the thermal bleaching studies, for which a range of temperatures from 300 to 77 K can be achieved with an accuracy of ± 0.2 °C. Details of the nanosecond-to-subnanosecond lifetime measurements have been described in our previous reports.¹⁵ In brief, the fundamental train of pulses from a Ti/sapphire oscillator (82 MHz, Spectra Physics) was used to produce second harmonics (375–425 nm) as an excitation light source. The emission signal was then detected by a time-correlated single-photon-counting system (Edinburgh OB900-L). After convolution, emission signal as fast as 80 ps is

confidently resolvable. The nanosecond transient absorption was recorded with a laser flash photolysis system (Edinburgh LP920) in which the third harmonic (355 nm) of an Nd:YAG laser and a white light square pulse were used as pump and probe beams, respectively. These two pulses were crossed at a 90° angle with an overlapping distance of 10 mm. The temporal resolution is limited by the excitation pulse duration of approximately 8 ns. Sample solution of ~ 6 mL was used in the ns transient absorption experiments. The steady-state absorption spectrum was recorded after measurement to ensure negligible decomposition during data acquisition.

2.3. Theoretical Approaches. The geometry of **1-CF** and its various open forms is optimized at the B3LYP/6-31G* theoretical level.¹⁶ We took into consideration the relative energies of these isomers by adding the solvation effect of CH₂Cl₂ via the CPCM model into the gas-phase ones. After the converged geometries are obtained, the vibrational frequency analysis is done to confirm that the number of the imaginary frequency is zero, which is expected to be the criterion of a minimum.

The dipole moment of the excited state is calculated by TDB3LYP/6-31G* on the basis of B3LYP/6-31G* geometry.¹⁷ According to Hellmann–Feynman theory, the dipole moment is the analytic derivative of the energy of the state with respect to an applied electric field. We thus calculate the excitation energy and ground-state energy upon applying the 0.001 au electric field from six directions (x , $-x$, y , $-y$, z , $-z$). The excited-state energy in each direction is calculated to be the excitation energy plus the ground-state energy. Taking a numerical derivative, as shown in eq 2, we can obtain each direction of the excited-state dipole moment

$$\mu(x) = \frac{E(x) - E(-x)}{F(x) - F(-x)} \quad (2)$$

where $E(x)$ is the excited-state energy in the x direction and $F(x)$ is the applied electric field strength in the x direction. All calculations were carried out using Gaussian03.^{18,19}

3. Results and Discussion

Photochromism of **1-CF** is supported by the changes of absorption spectra (in CH₂Cl₂) as a function of UV-excitation time. As shown in Figure 1a, upon 354 nm continuous irradiation, the lowest-lying absorption peak of **1-CF** at 384 nm gradually decreases, accompanied by the emergence of a new absorption band maximizing at 430 nm and extending to 550 nm. Ultimately, owing to light-induced reverse reaction together with thermal bleaching (vide infra), equilibrium, that is, a photostationary state, is reached regardless of further exposure to UV light. Figure 1b then demonstrates the 450 nm light-induced reverse reaction initiated from the photostationary state. Because absorption at 450 nm is negligible for **1-CF**, only **1-OF** is excited upon 450 nm irradiation. Clearly, as shown in Figure 1b, the absorption spectrum exclusively (>99%) returns to **1-CF**. Note that during the same irradiation period to prepare Figure 1b, the much slower thermal bleaching process of **1-OF** is considered to be negligible (vide infra). Such a reversible 354/450 nm switching process can be proceeded at least 10 cycles with only $\sim 2.5\%$ loss, as indicated by the recovery of the 384 nm absorption band of **1-CF** (inset of Figure 1), implying good photostability of compound **1** during the photoinduced forward and reverse processes.

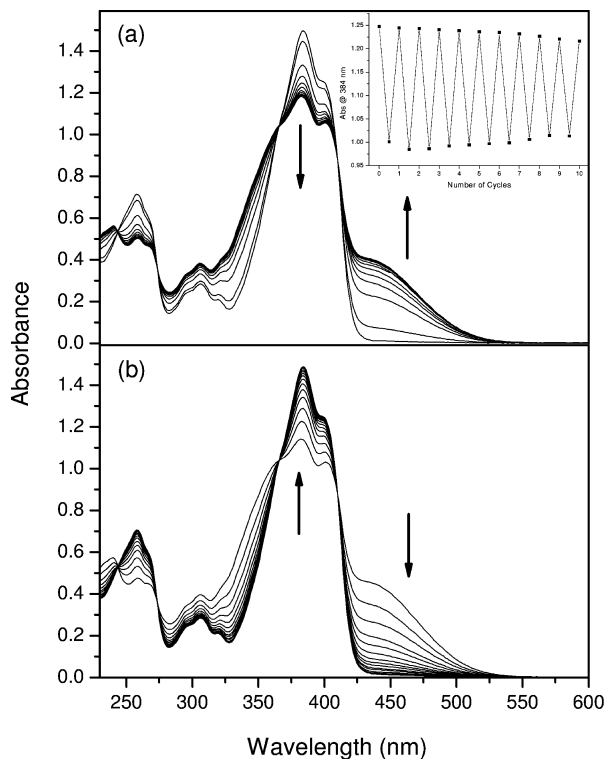


Figure 1. UV-vis absorption spectra of **1** in CH_2Cl_2 at room temperature obtained with different exposure times, 0 to 390 s, with increments of 30 s, under continuous irradiation of (a) 354 nm followed by (b) 450 nm with the same time course. Inset: Absorbance at 384 nm monitored in the first 10 photochromic cycles, in which each cycle consists of 15 min of 354 nm irradiation followed by 40 min of 450 nm irradiation.

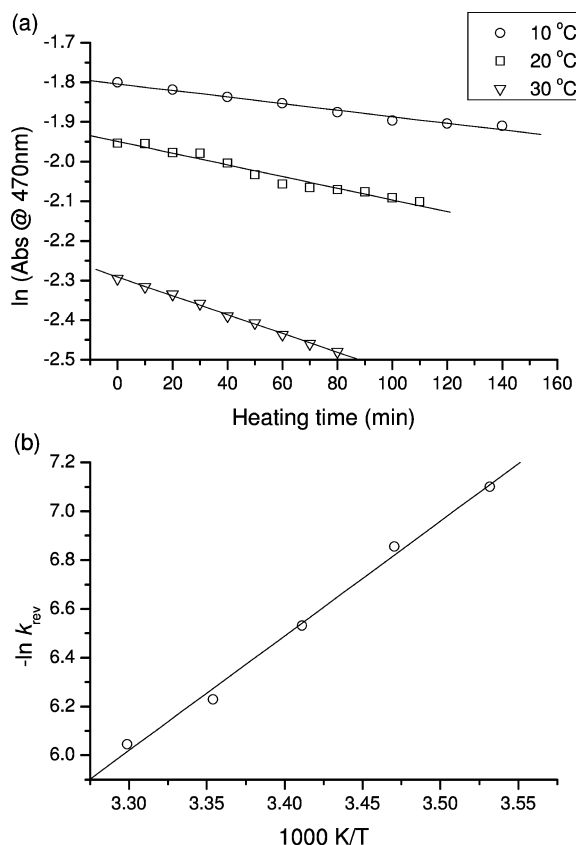
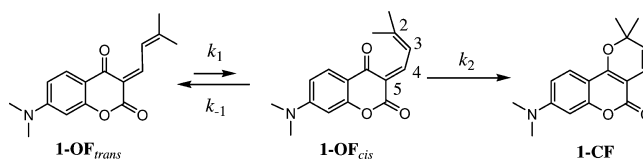


Figure 2. Compound **1-OF** in CH_2Cl_2 . (a) Plot of $\ln A_{470\text{nm}}$ versus reaction time at various temperatures. (b) Plot of $\ln k_{\text{rev}}$ versus $1/T$. See the text for details.

SCHEME 2: Sequential Thermal Bleaching Reaction of **1**



We then inspected the **1-OF** \rightarrow **1-CF** thermal bleaching by monitoring the decrease in absorbance of **1-OF** (e.g., 470 nm) in the dark at various temperatures. Straight line plots of the logarithm of absorbance versus reaction time (Figure 2a) evidence the first-order kinetics. Taking k_{rev} to be the rate constant for the reverse reaction, an Arrhenius plot of $\ln k_{\text{rev}}$ as a function of $1/T$ reveals a straight line (Figure 2b). Consequently, activation energy and frequency factor for the **1-OF** \rightarrow **1-CF** thermal bleaching process are calculated to be 58.2 kJ/mol and $1.7 \times 10^5 \text{ s}^{-1}$, respectively, in CH_2Cl_2 . To rationalize the result, we tentatively propose a mechanism for the **1-OF** \rightarrow **1-CF** thermal bleaching reverse reaction on the basis of a sequential reaction shown in Scheme 2, incorporating the reactant **1-OF**_{trans}, the intermediate (or activated complex) **1-OF**_{cis}, and the product **1-CF**.

On one hand, if the **1-OF**_{cis} \rightarrow **1-CF** process has a negligible barrier (or barrierless), then either k_2 or k_{-1} is $\gg k_1$. In this case, **1-OF**_{cis} may be considered to be an activated complex, and the overall reaction kinetics can be treated as a typical Arrhenius pattern, expressed as

$$k_{\text{rev}} = \frac{k_1 k_2}{k_{-1} + k_2} \leq k_1 = A e^{-E_a/RT} \quad (3)$$

using the steady-state approximation, where E_a denotes the activation energy for **1-OF**_{trans} \rightarrow **1-OF**_{cis} isomerization. On the other hand, if k_2 is relatively slow, that is, $k_2 \ll k_1$, then **1-OF**_{cis} can be treated as an intermediate, and the overall reaction kinetics is expressed as

$$k_{\text{rev}} = \frac{k_1}{k_{-1}} k_2 = k_2 e^{-\Delta G^\ddagger/RT} = A e^{-\Delta E_2/RT} e^{-\Delta G^\ddagger/RT} = A e^{-(\Delta E_2 + \Delta G^\ddagger)/RT} \quad (4)$$

assuming that **1-OF**_{trans} and **1-OF**_{cis} are in fast equilibrium, where ΔG^\ddagger and ΔE_2 are the difference in thermal energy between **1-OF**_{trans} and **1-OF**_{cis} and the activation energy for the **1-OF**_{cis} \rightarrow **1-CF** process, respectively. At first glance, it seems that both kinetic expressions can explain the straight line plot of $\ln k_{\text{rev}}$ versus $1/T$ well. Nevertheless, for the former process, the frequency factor is expected to be small because of the entropy-unfavorable **1-OF**_{trans} \rightarrow **1-OF**_{cis} rotational process. Conversely, the pre-exponential factor, A , for the latter process should correlate with certain vibrational frequencies on the order of $>10^{10} \text{ s}^{-1}$. Accordingly, the small frequency factor of $1.7 \times 10^5 \text{ s}^{-1}$ extracted experimentally leads us to propose the former to be a more plausible pathway, implying that the **1-OF**_{cis} \rightarrow **1-CF** process may be subject to a rather small or even negligible barrier. Note that the frequency factor is smaller than those of diphenyl-substituted chromenes by more than one order of magnitude.^{2,10,11} This may be due to the fact that the phenyl groups in chromenes stabilize planar conformation via extended conjugation, forming a preorganized structure with *s-cis* geometry, whereas dimethyl groups in **1-OF** cannot restrict the

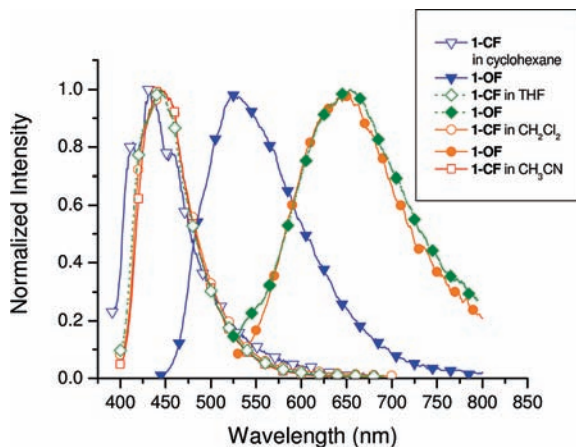


Figure 3. Emission spectra of **1-CF** and **1-OF** in cyclohexane, THF, CH_2Cl_2 , and CH_3CN at room temperature. Note the **1-OF** emission in CH_3CN was not observable. The excitation wavelengths are 370 and 450 nm for **1-CF** (before irradiation) and **1-OF** (in the photostationary state), respectively. See the text for detail.

TABLE 1: Selected Photophysical Properties of 1-CF and 1-OF in CH_2Cl_2

	UV-vis absorption maxima (nm) (ϵ , $10^3 \text{ M}^{-1} \text{ cm}^{-1}$)	photoluminescence maxima (nm)	quantum yield	observed lifetime (ps)
1-CF	384 (56.4), 399 (47.7)	445	0.095	260
1-OF	430 (37.2), 470 (21.8)	649	0.0058	93
2-CF	390 (35.3), 404 (29.7)	463	0.026	76
2-OF	419 (34.0), 450 (22.4)	N/A	N/A	N/A
3-CF	392 (85.0), 409 (74.4)	458	0.023	75

C2–C3 and C4–C5 double bonds in coplanarity as efficiently, resulting in the reduction of entropic factor for the **1-OF_{cis}** formation. The 58.2 kJ/mol activation energy of the **1-OF_{trans}** \rightarrow **1-OF_{cis}** process extracted experimentally may be rationalized by strong steric effect between the carbonyl group and the dimethyl substituents in the **1-OF_{cis}** conformer.

Among most photochromic systems, compound **1** possesses a remarkable feature in that the fluorescence for both isomers is well resolved. Upon 370 nm excitation of freshly prepared **1-CF** in which no interference of **1-OF** exists, as shown in Figure 3, an emission band maximizing at 445 nm was promptly observed. Conversely, at the photostationary state, with 450 nm excitation of **1-OF** (i.e., the **1-OF_{trans}** form), a 650 nm fluorescence band was well resolved in CH_2Cl_2 . (See Figure 3.) Table 1 lists the photophysical parameters for both forms in CH_2Cl_2 . It is noteworthy that the fluorescence quantum yields of 0.095 and 0.0058 for **1-CF** and **1-OF** are considerably higher than those of the majority of photochromes bearing pyran moieties,^{2,10,11} especially the OF isomers. By using the time-correlated single-photon-counting technique, the lifetimes of **1-CF** and **1-OF** in CH_2Cl_2 were measured to be 260 ± 15 (monitored at 470 nm) and 90 ± 15 ps (monitored at 680 nm). Two distinctly different lifetimes imply that the lowest excited states of **1-CF** and **1-OF** are not in equilibrium. It is also worthy to note that at the photostationary state (e.g., Figure 1a acquired at 390 s irradiation time), upon monitoring at the **1-OF** emission of 650 nm, the excitation spectrum attributed to **1-CF** is negligible. Furthermore, when performing lifetime measurements, we also made attempts to monitor the formation of **1-OF** at 700 nm emission while exclusively exciting **1-CF** with 380 nm and failed to resolve the ~ 90 ps decay of **1-OF**. The results unambiguously conclude that the photoinduced formation of **1-OF**; that is, **1-CF*** \rightarrow **1-OF** (* denotes the electronically

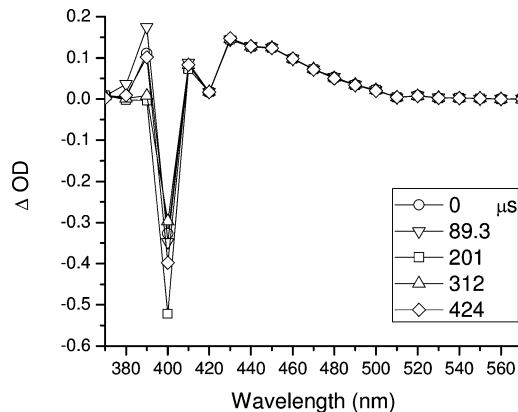


Figure 4. Time-dependent nanosecond transient absorption spectra of **1-CF** in CH_2Cl_2 .

excited state) is a nonadiabatic process (from the electronically excited **1-CF** to the ground-state **1-OF** PES).

To investigate the photochromic dynamics further, we evaluated the conversion efficiencies of both the forward and reverse reactions. The **1-CF*** \rightarrow **1-OF** forward reaction was monitored with an Nd/YAG pumped Ti/sapphire laser tuned to 384 nm, in which the absorption attributed to **1-OF** was minimized, whereas it was maximized for **1-CF**; the **1-OF*** \rightarrow **1-CF** reverse reaction was monitored with a 488 nm Argon laser to avoid the **1-CF** absorption. Under a fixed volume, V , of solution with vigorous stirring, the optical density at 470 nm ($A_{470\text{nm}}$) was recorded in a cuvette of optical path length, b , before and after an illumination period of 30 s, during which the thermal reaction was negligible. Taking the ratio of the number of product molecules generated versus the number of photons absorbed, using

$$\frac{V\Delta A_{470} \epsilon b}{\sum_t [P_0 - P(t)] \Delta t / h\nu} \quad (5)$$

where P_0 stands for the transmitted laser intensity as blank CH_2Cl_2 solution in the same cuvette was placed on the beam path and P stands for the transmitted intensity recorded every 3 s during irradiation of the samples, the yields of the forward and reverse reactions were estimated to be 0.40 and 1.0%, respectively.

To gain further insight into the ring-opening mechanism, transient absorption measurements were performed with a 355 nm Nd/YAG (3rd harmonic) pump laser and a pulsed xenon arc probe. The results shown in Figure 4 reveal an apparent bleaching signal with negative ΔOD value around 400 nm, which unambiguously correlates with the depletion of ground-state **1-CF**. In addition, an absorption band appearing at 420–520 nm qualitatively matches the absorption spectral feature of **1-OF** well. In this study, the **1-OF** transient absorption held constant during a time delay of as long as 500 μs , which is consistent with the much longer recovery time for the **1-OF_{trans}** \rightarrow **1-CF** reverse process. Likewise, the **1-CF** bleaching band intensity remained nearly constant within this time period. Note that the fluctuation in intensity may plausibly be attributed to the **1-CF** stimulated emission overlapping in this region. In sum, except for the **1-OF_{trans}** product, this study showed no evidence of any other transient species with a lifespan of >8 ns. The result further supports the rate-determining **1-OF_{trans}** \rightarrow **1-OF_{cis}** process proposed earlier based on kinetic approaches.

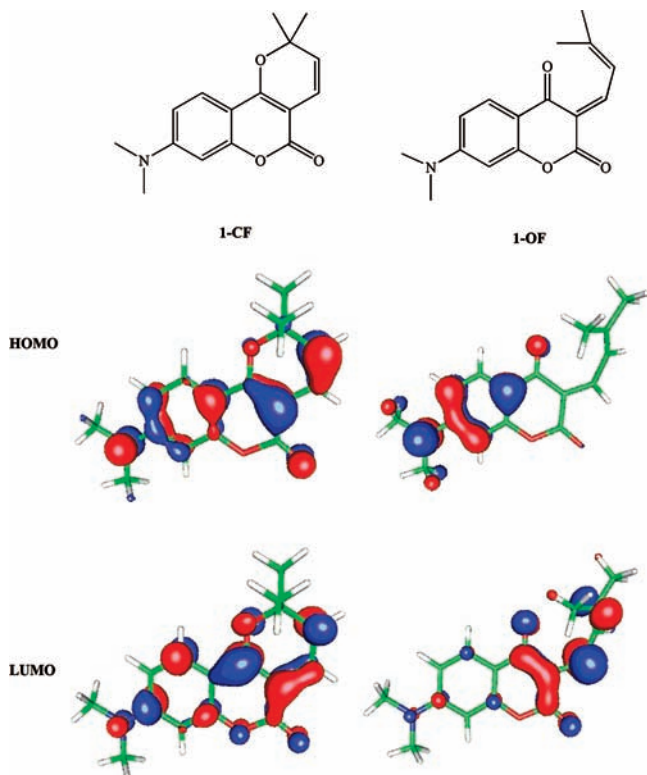


Figure 5. Structures and HOMO/LUMO contributed to the lowest-lying transition for **1-CF** and **1-OF**.

Furthermore, ring-opening is assumed to proceed, in part, at either the vibrationally excited S_1 (**1-CF**) or the highly electronically excited state (S_n , $n \geq 2$) because the conversion efficiency is found to be wavelength-dependent. In addition to 384 nm excitation with efficiency of 0.40%, the forward reaction conversion efficiency was also evaluated at excitation wavelengths of 410 and 355 nm, and the results were 0.26 and 0.51%, respectively. If C–O bond cleavage occurred at the thermally equilibrated level ($\nu = 0$) of S_1 (**1-CF**), then the conversion efficiency would have been the same regardless of excitation energy. Consequently, following excitation at higher lying states, it is believed that leaking channels through ring-opening take place during internal conversion, vibrational relaxation, or both, and these kinetic parameters are intrinsically inseparable. This finding is consistent with picosecond transient absorption measurements conducted by Kodama et al.,²⁰ showing that the spectral evolution differed while the pump wavelength was changed from 295 to 266 nm. Moreover, this explains the observation that fluorescence quantum yields decrease for certain naphthopyrans upon increasing the excitation wavelength^{2,11} because the ring-opening reaction becomes more prominent at higher energy levels.

Supplementary information regarding photophysical properties and reaction thermodynamics are provided via computational approaches. The results show that **1-OF**, compared with **1-CF**, bears considerable charge-transfer character from the donor site, the phenylamine moiety, to the acceptor, the pyran moiety in the excited state. (See Figure 5.) The orientations of respective dipole moments for **1-CF** and **1-OF**_{trans} are illustrated in Figure 6, in which yellow and red vectors represent dipole moments in S_0 and S_1 states, respectively. Obviously, there is a significant change in the dipole moment in terms of orientation and magnitude between S_0 and S_1 for **1-OF**_{trans}, as evidenced by the calculated value of as large as 14.33D. Conversely, the change in dipole moment (S_0 versus S_1) is only 0.87D for **1-CF**.

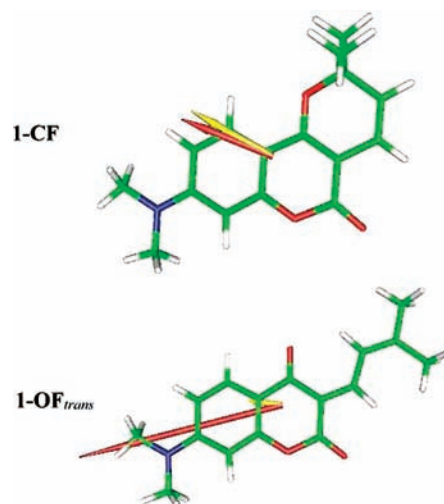
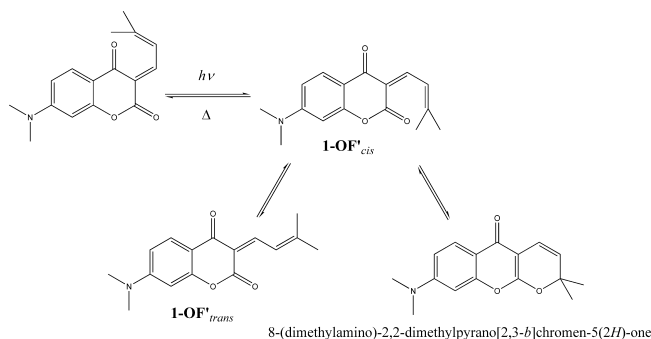


Figure 6. Calculated dipole moment vectors for **1-CF** and **1-OF**_{trans}, where yellow and red arrows indicate those of S_0 and S_1 , respectively.

SCHEME 3: Other Possible Isomers of **1-OF**



Accordingly, the emission gap of **1-OF**_{trans} is expected to be subject to changes in solvent polarity. This viewpoint is firmly supported by the remarkable solvatochromic behavior of **1-OF**_{trans} fluorescence, for which the peak wavelength shifts significantly from 526 nm in cyclohexane to as long as 649 nm in CH_2Cl_2 . (See Figure 3.) Note that we expected to observe even further red shift of **1-OF**_{trans} emission in CH_3CN . Unfortunately, the emission in CH_3CN was too weak to be resolved, conceivably because of the smaller energy gap such that quenching of emission via high frequency vibrational modes, that is, the so-called energy gap law,²¹ was fully operative. In agreement with the calculation, the **1-CF** emission maxima in cyclohexane (432 nm), THF (443 nm), CH_2Cl_2 (445 nm), and CH_3CN (445 nm) remain nearly unchanged, supporting similar dipolar vectors between the ground and excited states of **1-CF**. The calculation results also bring up three additional remarks: (1) As shown in Figure 6, the **1-OF**_{trans} S_0 dipole moment points to essentially the same direction as that of **1-CF** S_1 , facilitating a nonadiabatic channel for energy relaxation. (2) Clearly, as depicted in Figure 5, the LUMO of **1-CF** involves antibonding character of the C–O bond, manifesting the photoinduced ring-opening. (3) Compared with previously synthesized nonfluorescent CF analogues,^{9,22} the HOMO and LUMO of **1-CF** are calculated to have significant overlap, the result of which may increase the transition dipole and hence results in fluorescence as experimentally observed.

Similar to other photochromic compounds,^{20,23} we are also skeptical that a second-photon excitation of the generated **1-OF** may lead to double-bond flipping, producing conformers **1-OF'**_{cis} and **1-OF'**_{trans} shown in Scheme 3. However, thermal

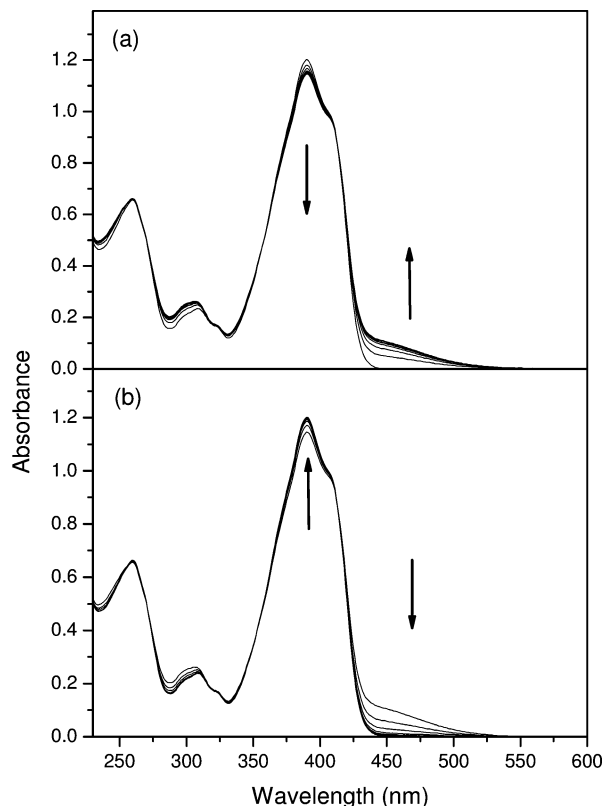


Figure 7. UV-vis absorption spectra of **2** in CH_2Cl_2 at room temperature obtained at different exposure times (0–600 s, an increment of 60 s) under continuous irradiation of (a) 354 nm, followed by (b) 450 nm for 540 s.

bleaching of **1-OF_{trans}** is relatively slow (Figure 2), whereas the lifetimes of these minor species are expected to be even longer according to a two-stage reversion process, that is, double-bond flipping, followed by ring-closure. As a result, lifetimes of **1-OF_{cis}** and **1-OF_{trans}** could not be precariously deconvoluted from the thermal bleaching time trace. Likewise, the possible formation of 8-(dimethylamino)-2,2-dimethylpyrano[2,3-*b*]chromen-5(2H)-one (Scheme 3) cannot be excluded in this study. Calculations, however, show that S_0 of 8-(dimethylamino)-2,2-dimethylpyrano[2,3-*b*]chromen-5(2H)-one is 36.5 kJ/mol higher in energy than **1-CF**, whereas **1-OF_{cis}** and **1-OF_{trans}** are at 41.1 and 8.54 kJ/mol, respectively, indicating that the cycloreversion byproduct may not be in an energy minimum. Nevertheless, further experiments have to be carried out to support this viewpoint.

Further fine-tuning of the colorant via R_1 , R_2 , or R_3 substituents (Scheme 1) is synthetically feasible to give compounds **2** and **3**. Pertinent absorption, emission, and dynamics data for **2** and **3** are also summarized in Table 1. The addition of a phenyl ring (**2**) and bromine (**3**) only slightly shifts the $S_0 \rightarrow S_1$ absorption maximum of **2-CF** and **3-CF** to 390 and 392 nm, respectively (cf. 384 nm in **1-CF**). The lack of spectral changes upon varying the substituents indicates that the designated functional groups are not directly attached to the chromophores involved in the transition. Support of this viewpoint is rendered by the time-dependent DFT, of which the result indicates that the electron density at R_1 , R_2 , and R_3 is not involved in either HOMO or LUMO. For instance, similar photochromic phenomena are observed for compound **2**. As shown in Figure 7, the forward and reverse reactions facilitated with 354/450 nm irradiation are evident with less pronounced absorption change compared with **1**.

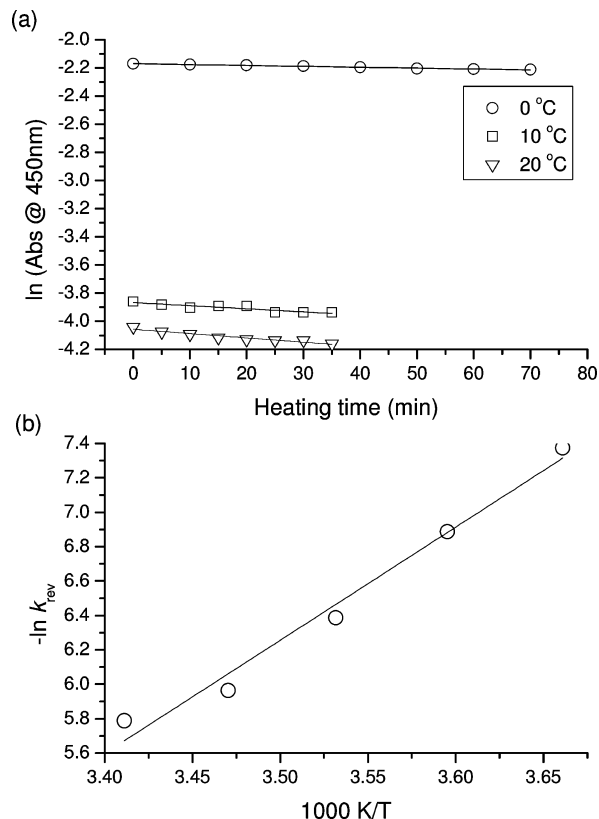
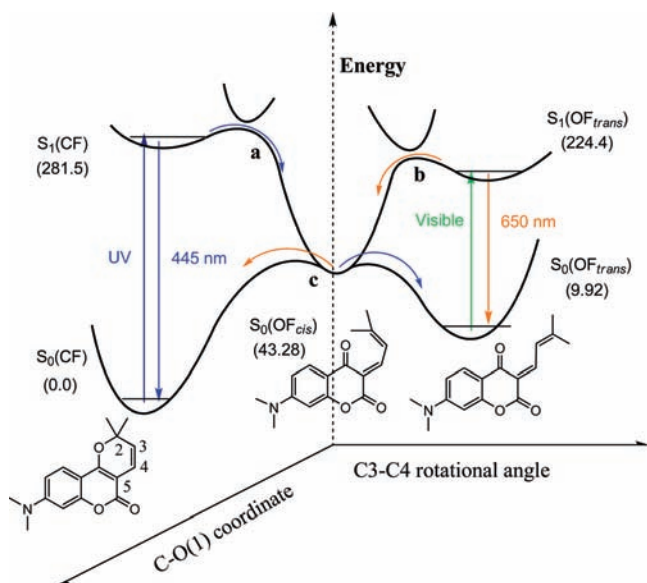


Figure 8. Compound **2-OF** in CH_2Cl_2 . (a) Plot of $\ln A_{450\text{nm}}$ versus reaction time at various temperatures. (b) Plot of $\ln k_{\text{rev}}$ versus $1/T$.

Thermal bleaching of **2-OF** was also studied (Figure 8), and the activation energy of **2-OF** \rightarrow **2-CF** was determined to be 54.8 kJ/mol. The associated frequency factor of $3.6 \times 10^5 \text{ s}^{-1}$ is not substantially larger than that of **1-OF**. Accordingly, structural factors other than the absence of planar orienting phenyl substituents at the R_1 and R_2 positions contribute to the relatively low frequency factor of **1** compared with common phenyl-substituted chromenes. Intriguingly, the substitution, to a certain extent, does affect the ring-opening kinetics. Upon replacing $R_3 = \text{H}$ by $R_3 = \text{Br}$, compound **3**, which exclusively exists as the closed form (**3-CF**) in the ground state, to our surprise, does not undergo photochromic reaction, as indicated by negligible changes of the absorption spectrum after a prolonged (2 h) 354 nm (0.2 W/cm^2) photolysis. As for a prompt interpretation, because of the electron-withdrawing property of the bromine substituent, the result may be rationalized by the destabilization of activated complex and hence a high energy barrier for the **3-CF*** \rightarrow **3-OF_{cis}** reaction. (See intersection a in Scheme 4.) Alternatively, as evidenced by the fast decay rate of **3-CF** fluorescence (Table 1), the results are tentatively rationalized by other fast radiationless channels, for example, heavy-atom-induced intersystem crossing and so on, which dominate the deactivation process of **3-CF** upon excitation.

According to the above Results and Discussion, we reasonably propose an overall photochromic reaction of compound **1** illustrated in Scheme 4. The ring-opening reaction pathway is constructed according to a commonly acknowledged crossing from the S_1 PES of CF to the S_0 of OF.^{8,22,24–26} Subsequent to excitation, the CF undergoes C–O bond cleavage, from which it evolves toward the ground state of the *ortho*-quinodial product with an *s-cis* geometry, $S_0(\text{OF}_{\text{cis}})$, perhaps through a conical intersection. C3–C4 single bond rotation then follows to generate the more stable *s-trans* OF. Similarly, the cyclization reaction occurs via the intersection of $S_1(\text{OF}_{\text{trans}})$ and $S_0(\text{OF}_{\text{cis}})$,

SCHEME 4: Proposed Photochromism Mechanisms of **1**^a

^a Energy levels (in parentheses) are in kilojoules per mole. Relative energies in the ground state are estimated via computation, whereas those in the excited state are obtained simply by the addition of the energy gap measured from absorption onsets in CH₂Cl₂.

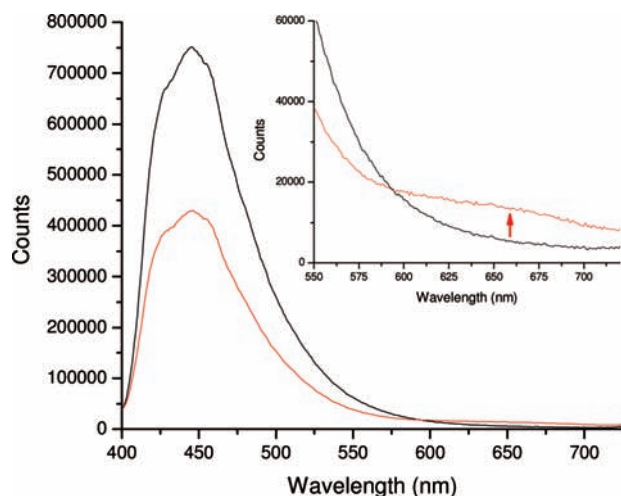


Figure 9. Emission spectra of **1-CF** (black line) and its photostationary state with **1-OF** (red line) in CH₂Cl₂ upon irradiation with 366 nm light for 15 min. Insert: Enlargement of **1-OF** emission.

followed by relaxation to S₀(CF). In this model, there is a lack of equilibrium between S₁(CF) and S₁(OF_{trans}), as supported by their distinctly different lifetimes. (See Table 1, *vide supra*.)

4. Conclusions

In conclusion, we have performed comprehensive thermodynamic and kinetic studies regarding the photo- and thermo-chromism of a series of colorants **1–3** bearing pyrano[3,2-*c*]chromen-5-one moiety. In particular, compound **1** enables dual fluorescence detection while it exhibits photochromism in both directions. In view of application, the viability of **1** in, for example, data storage is perspective, owing to its relatively slow thermal reversion compared with most photochromic naphthopyran derivatives,^{2,10,11} which is the result of a smaller frequency factor. For a preliminary test, the ratios of emission intensity at 649 nm (*I*₆₄₉) versus 445 nm (*I*₄₄₅) for **1-CF** and the photostationary state are taken with 366 nm excitation, which coincides

with an isosbestic point. The *I*₆₄₉/*I*₄₄₅ value for the photostationary state is about four times as large as that of **1-CF** alone. (See Figure 9.) In the current stage, because of the relatively low emission quantum yield of, for example, **1-OF**, the on/off ratio between **1-CF** and **1-OF** fluorescence in this coumarin series is not high enough for practical use. This disadvantage is expected to be circumvented by substituting coumarin moiety with other stronger emitters such as xanthene, flavone, and so on. As a result, by optimizing the structure to further reduce the thermal bleaching rate while retaining fluorescence, optimal single-layered data storage devices can be crafted.

Acknowledgment. This work was funded by the National Science Council of Taiwan, R.O.C. We are also grateful to the National Center for High-Performance Computing for computer time and facilities.

References and Notes

- (1) Crano, J. C.; Guglielmetti, R. J. *Organic Photochromic and Thermo-chromic Compounds*; Plenum Press: New York, 1999.
- (2) di Nunzio, M. R.; Gentili, P. L.; Romani, A.; Favaro, G. *Chem-PhysChem* **2008**, *9*, 768.
- (3) (a) Ottavi, G.; Favaro, G.; Malatesta, V. J. *Photochem. Photobiol., A* **1998**, *115*, 123. (b) Favaro, G.; Malatesta, V.; Mazzucato, U.; Ottavi, G.; Romani, A. *J. Photochem. Photobiol., A* **1995**, *87*, 235.
- (4) (a) Görner, H. *Phys. Chem. Chem. Phys.* **2001**, *3*, 416. (b) Chibisov, A. K.; Görner, H. *J. Phys. Chem. A* **1997**, *101*, 4305.
- (5) Oliveira, M. M.; Salvador, M. A.; Coelho, P. J.; Carvalho, L. M. *Tetrahedron* **2005**, *61*, 1681.
- (6) Sakata, T.; Jackson, D. K.; Mao, S.; Marriott, G. *J. Org. Chem.* **2008**, *73*, 227.
- (7) Bao, Z.; Ng, K.-Y.; Yam, V. W.-W.; Ko, C.-C.; Zhu, N.; Wu, L. *Inorg. Chem.* **2008**, *47*, 8912.
- (8) Moine, B.; Buntinx, G.; Poizat, O.; Rehaut, J.; Moustrou, C.; Samat, A. *J. Phys. Org. Chem.* **2007**, *20*, 936.
- (9) Yang, D.-Y.; Chen, Y.-S.; Kuo, P.-Y.; Lai, J.-T.; Jiang, C.-M.; Lai, C.-H.; Liao, Y.-H.; Chou, P.-T. *Org. Lett.* **2007**, *9*, 5287.
- (10) Jockusch, S.; Turro, N. J.; Blackburn, F. R. *J. Phys. Chem. A* **2002**, *106*, 9236.
- (11) Ortica, F.; Bougdid, L.; Moustrou, C.; Mazzucato, U.; Favaro, G. *J. Photochem. Photobiol., A* **2008**, *200*, 287.
- (12) Liu, H.-h.; Chen, Y. *J. Phys. Chem. A* **2009**, *113*, 5550.
- (13) Huang, C.-N.; Kuo, P.-Y.; Lin, C.-H.; Yang, D.-Y. *Tetrahedron* **2007**, *63*, 10025.
- (14) (a) Jones, G.; Jackson, W. R.; Choi, C. Y.; Bergmark, W. R. *J. Phys. Chem.* **1985**, *89*, 294. (b) Drake, J. M.; Lesiecki, M. L.; Camaioni, D. M. *Chem. Phys. Lett.* **1985**, *113*, 530. (c) Lakowicz, J. R. *Principles of Fluorescence Spectroscopy*; Plenum Press: New York, 1983.
- (15) (a) Chou, P.-T.; Yu, W.-S.; Cheng, Y.-M.; Pu, S.-C.; Yu, Y.-C.; Lin, Y.-C.; Huang, C.-H.; Chen, C.-T. *J. Phys. Chem. A* **2004**, *108*, 6487. (b) Chou, P.-T.; Chen, Y.-C.; Yu, W.-S.; Chou, Y.-H.; Wei, C.-Y.; Cheng, Y.-M. *J. Phys. Chem. A* **2001**, *105*, 1731.
- (16) Becke, A. D. *J. Chem. Phys.* **1993**, *98*, 5648.
- (17) (a) Jamorski, C.; Casida, M. E.; Salahub, D. R. *J. Chem. Phys.* **1996**, *104*, 5134. (b) Petersilka, M.; Gossmann, U. J.; Gross, E. K. *U. Phys. Rev. Lett.* **1996**, *76*, 1212. (c) Bauernschmitt, R.; Ahlrichs, R.; Hennrich, F. H.; Kappes, M. M. *J. Am. Chem. Soc.* **1998**, *120*, 5052. (d) Casida, M. E. *J. Chem. Phys.* **1998**, *108*, 4439. (e) Stratmann, R. E.; Scuseria, G. E.; Frisch, M. J. *J. Chem. Phys.* **1998**, *109*, 8218. (f) Lee, C.; Yang, W.; Parr, R. G. *Phys. Rev. B* **1988**, *37*, 785.
- (18) Frisch M. J.; Trucks, G. W.; Schlegel, H. B.; Scuseria, G. E.; Robb, M. A.; Cheeseman, J. R.; Montgomery, J. A., Jr.; Vreven, J. T.; Kudin, K. N.; Burant, J. C.; Millam, J. M.; Iyengar, S. S.; Tomasi, J.; Barone, V.; Mennucci, B.; Cossi, M.; Scalmani, G.; Rega, N.; Petersson, G. A.; Nakatsuji, H.; Hada, M.; Ehara, M.; Toyota, K.; Fukuda, R.; Hasegawa, J.; Ishida, M.; Nakajima, T.; Honda, Y.; Kitao, O.; Nakai, H.; Klene, M.; Li, X.; Knox, J. E.; Hratchian, H. P.; Cross, J. B.; Bakken, V.; Adamo, C.; Jaramillo, J.; Gomperts, R.; Stratmann, R. E.; Yazyev, O.; Austin, A. J.; Cammi, R.; Pomelli, C.; Ochterski, J. W.; Ayala, P. Y.; Morokuma, K.; Voth, G. A.; Salvador, P.; Dannenberg, J. J.; Zakrzewski, V. G.; Dapprich, S.; Daniels, A. D.; Strain, M. C.; Farkas, O.; Malick, D. K.; Rabuck, A. D.; Raghavachari, K.; Foresman, J. B.; Ortiz, J. V.; Cui, Q.; Baboul, A. G.; Clifford, S.; Cioslowski, J.; Stefanov, B. B.; Liu, G.; Liashenko, A.; Piskorz, P.; Komaromi, I.; Martin, R. L.; Fox, D. J.; Keith, T.; Al-Laham, M. A.; Peng, C. Y.; Nanayakkara, A.; Challacombe, M.; Gill, P. M. W.; Johnson, B.; Chen, W.; Wong, M. W.; Gonzalez, C.; Pople, J. A. *Gaussian 03*, revision D.01; Gaussian, Inc.: Wallingford, CT, 2004.

(19) Yu, J.-K.; Cheng, Y.-M.; Hu, Y.-H.; Chou, P.-T.; Chen, Y.-L.; Lee, S.-W.; Chi, Y. *J. Phys. Chem. B* **2004**, *108*, 19908.

(20) Kodama, Y.; Nakabayashi, T.; Segawa, K.; Hattori, E.; Sakuragi, M.; Nishi, N.; Sakuragi, H. *J. Phys. Chem. A* **2000**, *104*, 11478.

(21) (a) Chen, K.-Y.; Hsieh, C.-C.; Cheng, Y.-M.; Lai, C.-H.; Chou, P. T. *Chem. Commun.* **2006**, 4395. (b) Siebrand, W. *J. Chem. Phys.* **1967**, *47*, 2411.

(22) Chen, J.-R.; Wong, J.-B.; Kuo, P.-Y.; Yang, D.-Y. *Org. Lett.* **2008**, *10*, 4823.

(23) Gentili, P. L.; Ortica, F.; Favaro, G. *J. Phys. Chem. B* **2008**, *112*, 16793.

(24) Gentili, P. L.; Danilov, E.; Ortica, F.; Rodgers, M. A. J.; Favaro, G. *Photochem. Photobiol. Sci.* **2004**, *3*, 886.

(25) Antipin, S. A.; Petrukhin, A. N.; Gostev, F. E.; Marevtsev, V. S.; Titov, A. A.; Barachevsky, V. A.; Strokach, Y. P.; Sarkisov, O. M. *Chem. Phys. Lett.* **2000**, *331*, 378.

(26) (a) Celani, P.; Bernardi, F.; Olivucci, M.; Robb, M. A. *J. Am. Chem. Soc.* **1997**, *119*, 10815. (b) Migani, A.; Gentili, P. L.; Negri, F.; Olivucci, M.; Romani, A.; Favaro, G.; Becker, R. S. *J. Phys. Chem. A* **2005**, *109*, 8684.

JP904076S